ARTICLE

BIOTECHNOLOGY and BIOENGINEERING

Rapid Strain Improvement Through Optimized Evolution in the Cytostat

Alan Gilbert,[1,2] Dipen P. Sangurdekar,[1,2] Friedrich Srienc[1,2]

[1]Department of Chemical Engineering and Materials Science, University of Minnesota, 151 Amundson Hall, 421 Washington Avenue S.E., Minneapolis, Minnesota 55455-0312

[2]BioTechnology Institute, University of Minnesota, 240 Gortner Laboratory, 1479 Gortner Avenue, St. Paul, Minnesota 55108; telephone: 612-624-9776; fax: 612-625-1700; e-mail: srienc@umn.edu

Received 11 August 2008; revision received 10 December 2008; accepted 12 January 2009

Published online 20 January 2009 in Wiley InterScience (www.interscience.wiley.com). DOI 10.1002/bit.22272

ABSTRACT: Acetate is present in lignocellulosic hydrolysates at growth inhibiting concentrations. Industrial processes based on such feedstock require strains that are tolerant of this and other inhibitors present. We investigated the effect of acetate on *Saccharomyces cerevisiae* and show that elevated acetate concentrations result in a decreased specific growth rate, an accumulation of cells in the G1 phase of the cell cycle, and an increased cell size. With the cytostat cultivation technology under previously derived optimal operating conditions, several acetate resistant mutants were enriched and isolated in the shortest possible time. In each case, the isolation time was less than 5 days. The independently isolated mutant strains have increased specific growth rates under conditions of high acetate concentrations, high ethanol concentrations, and high temperature. In the presence of high acetate concentrations, the isolated mutants produce ethanol at higher rates and titers than the parental strain and a commercial ethanol producing strain that has been analyzed for comparison. Whole genome microarray analysis revealed gene amplifications in each mutant. In one case, the *LPP1* gene, coding for lipid phosphate phosphatase, was amplified. Two mutants contained amplified *ENA1*, *ENA2*, and *ENA5* genes, which code for P-type ATPase sodium pumps. *LPP1* was overexpressed on a plasmid, and the growth data at elevated acetate concentrations suggest that *LPP1* likely contributes to the phenotype of acetate tolerance. A diploid cross of the two mutants with the amplified *ENA* genes grew faster than either individual haploid parent strain when 20 g/L acetate was supplemented to the medium, which suggests that these genes contribute to acetate tolerance in a gene dosage dependent manner.

Biotechnol. Bioeng. 2009;103: 500–512.

KEYWORDS: robust strains; evolution; cytostat; *Saccharomyces cerevisiae*; lignocellulosic ethanol

Introduction

Rapid growth and product formation rates are of practical significance to industrial biotechnology as shorter cultivation times lead to higher productivity. In the case of industrial ethanol production using lignocellulosic feedstocks, ethanol production is severely affected by the presence of growth inhibitors in the feed mixture (Hahn-Hägerdal et al., 2007; Stephanopoulos, 2007). These inhibitors include acetate, furfural, aromatics, and other organics (Aden et al., 2002; Hahn-Hägerdal et al., 1991; Mohagheghi et al., 2006). While it is in principle possible to remove these inhibitors through detoxification or separation processes (Buhner and Agblevor, 2004; Berson et al., 2005), it is better economically to not have to implement additional processing steps. The ideal microorganism would be able to grow quickly in the presence of the growth inhibitors present in a hydrolysate. It is clear that a rational implementation of mutations needed in a cell line to accomplish this is not possible as the required mutations are not known. Therefore evolutionary methods involving mutagenesis and selection must be employed to be successful.

We have previously described an optimal strategy for isolating mutants resistant to adverse growth conditions through the use of the cytostat (Gilbert and Srienc, 2009). The cytostat, a modification of the turbidostat method using automated flow cytometry to measure cell concentrations (Kacmar and Srienc, 2005; Kacmar et al., 2006), allows the culture to be maintained at such low cell densities that the culture's contribution to the environment is negligible. The selection condition imposed on the culture is precisely defined by the feed medium, and the specific growth rate can be adjusted by the supplementation of inhibitors to the feed medium such that the growth conditions match a previously developed optimal isolation strategy. Thus, the isolation time is minimized (Gilbert and Srienc, 2009). In contrast to

Correspondence to: F. Srienc

Additional Supporting Information may be found in the online version of this article.

a chemostat, the enrichment of a faster growing, more robust mutant is easily detected, as the measured dilution rate increases to match the specific growth rate of the culture when the mutant takes over the cell population.

Here we focus on the isolation of mutant strains of *Saccharomyces cerevisiae* that are resistant to high acetate concentrations. Acetate is present at high concentrations, even over 10 g/L acetate, in lignocellulosic hydrolysates (Klinke et al., 2003; Taherzadeh et al., 1997) and inhibits the growth of *S. cerevisiae* (Palmqvist et al., 1999; Pampulha and Loureiro-Davis, 1989). The cytostat cultivation technique enabled isolation of acetate tolerant strains of *S. cerevisiae* in less than 5 days. The mutant strains produce ethanol at higher titers and higher rates than both the parental strain and a commercially available ethanologenic strain. Analysis by cDNA microarrays revealed gene amplifications in each isolated mutant.

Materials and Methods

Strains and Growth Conditions

We used in this work *S. cerevisiae* wild type strain S288c (MATα SUC2 mal mel gal2 CUP1) and its isogenic variant of opposing mating type X2180-1A (MATa SUC2 mal mel gal2 CUP1) (Mortimer and Johnston, 1986). Strain X2180-1A was a kind gift from Dennis Livingston. We developed mutant strains AG3 and AG4, using S288c as a parental strain, and mutant AG5, using X2180-1A as a parental strain. A commercially available ethanologenic diploid strain, Ethanol Red (Fermentis, Marcq-en-Barœul, France), was used for comparison in the kinetic studies. Strain D603 (MATa/MATα *ura*3-52 *lys*2-801 *met his*3 *ade*2-101 *reg*1-501 [cir+]) (Srienc et al., 1986) was used to evaluate growth effects after overexpression of the *LPP1* gene. Strains were preserved long term by storage in 15% glycerol (Mallinckrodt Baker, Phillipsburg, NJ) at −80°C. Strains were streaked fresh from frozen stocks on to YPD agar plates (20 g/L glucose [Mallinckrodt Baker], 20 g/L peptone [Becton Dickinson, Sparks, MD], 10 g/L yeast extract [Becton Dickinson], 15 g/L agar [Matheson, Coleman, & Bell, Norwood, OH]). Single colonies were isolated from YPD agar plates and cultivated overnight in 50 mL of SD medium (20 g/L glucose, 6.7 g/L Difco Yeast Nitrogen Base w/o Amino Acids [Becton Dickinson]) at 30°C in a 250 mL Erlenmeyer flask with shaking at 250 rpm. These cultures served as inoculum cultures for continuous cultures. Strain D603 was grown on SD medium supplemented with 60 mg/L uracil, 150 mg/L lysine, 100 mg/L methionine, 80 mg/L histidine, and 100 mg/L adenine (all from Sigma–Aldrich, St Louis, MO). When D603 was transformed with plasmid pRS169 or pRS169-LPP1, uracil was omitted from the medium as both plasmids contain the *URA3* gene as the selection marker.

Cytostat

Cytostat operation (Kacmar et al., 2006) was carried out in either a 2 L BIOSTAT B or 2 L LH Fermentation bioreactor. Each continuous bioreactor initially contained approximately 300 mL of SD medium and was inoculated with 5 mL of overnight culture. The cytostat feed medium contained 5 g/L glucose and 6.7 g/L Difco yeast nitrogen base without amino acids, and the medium was supplemented with sodium acetate trihydrate (Sigma–Aldrich) as needed to reach the specified total acetate concentrations. All media were adjusted to pH 5.6 using 40% (v/v) H_3PO_4 (Sigma–Aldrich). The continuous cultures were maintained at the working volume of approximately 300 mL, aerated at 2 vvm, agitated at 300 rpm, and maintained at 30°C. Neither pH control nor dissolved oxygen control was used as the low cell density culture did not alter the pH of the feed medium and consumed negligible quantities of dissolved oxygen. Automated sampling and flow cytometric determination of the cell concentration and size distribution were performed as described previously (Kacmar et al., 2006). The cytostat cell number concentration was maintained at the specified set point of either 100,000 or 450,000 cells mL^{-1} using a controller gain of 0.0025 or 0.0008 $mL^2\,h^{-1}\,cells^{-1}$, respectively. Either a FACSCalibur (Becton-Dickinson Immunocytometry System, San Jose, CA) or an EasyCyte (Guava Technologies, Inc., Hayward, CA) flow cytometer was used for the single cell analysis.

Mutant Isolation

Mutant strains were isolated by plating samples of the cytostat effluent stream after the dilution rate had increased significantly. The YPD plates were incubated overnight at 30°C. Three single colonies were isolated and cultivated in SD medium overnight. Cultures were then transferred to SD medium supplemented with 20 g/L acetate and were screened for increased specific growth rates as compared to the specific growth rate of the wild type strain. The colony with the highest specific growth rate in each screen was preserved as the mutant strain.

Construction of Diploids

Mating of the mutated strains was performed on YPD agar plates. Each mutant strain was grown overnight at 30°C on an agar plate. Single colonies of each mutant were then mixed together on a fresh YPD plate (Burke and Stearns, 2000). After incubating overnight, the mixture was streaked on a fresh YPD plate to isolate individual colonies. Ten single colonies were isolated and had their ploidy verified by flow cytometry using the DNA staining protocol.

DNA Staining

For ploidy determination, exponential liquid cultures started from the single colonies were fixed in 70% (v/v) ethanol, washed in phosphate buffered saline (PBS, 8 g/L NaCl [Mallinckrodt Baker], 0.2 g/L KCl [JT Baker,

Phillipsburg, NJ], 2.7 g/L $Na_2HPO_4{\cdot}7H_2O$ [Mallinckrodt Baker], 0.24 g/L KH_2PO_4 [Fisher Scientific, Fair Lawn, NJ]), and then treated with 2 mg/mL RNase A (Sigma) for 2 h at 37°C in order to digest the cells' RNA. The cells were washed again in PBS, and then the cells' DNA was stained with 500 μg/mL propidium iodide (Sigma) for 30 min. Finally samples were diluted into PBS immediately before flow cytometric analysis. Propidium iodide fluorescence was measured using a band pass filter (585 ± 42 nm) on a FACSCalibur flow cytometer (Porro et al., 2003). Strains of known ploidy were used as controls.

For cell cycle distributions measurements, cells were cultivated on SD medium. Exponentially growing cells were centrifuged at 824 g for 15 min, washed in SD medium or SD medium supplemented with 20 g/L acetate, and then diluted into 50 mL of the same medium. After 4 h of growth at 30°C, samples were taken and the DNA distribution was determined using the described DNA staining protocol and flow cytometric analysis. Cell cycle analysis was performed in MultiCycle for Windows (Phoenix Flow Systems, San Diego, CA). All cultivations and analyses were performed in triplicate.

Microarray Analysis

Genomic DNA of wild type and mutant strains were isolated using standard DNA isolation methods (Burke and Stearns, 2000). The extracted and purified genomic DNA was sonicated (Branson Digital Sonifier, Danbury, CT) for 5-6 cycles of 10 seconds at a power setting of 40%. The resulting size of sonicated DNA had a median of 1 kb and a range of 0.5–1.4 kb. The DNA was subsequently stored at −20°C until further use. Sonicated DNA was labeled with Cy5 and Cy3-dUTP dyes (Amersham, Piscataway, NJ) using a genomic DNA labeling kit (BioPrime Array CGH labeling kit, Invitrogen, Carlsbad, CA). The labeled DNA was then purified using Microcon YM-30 columns (Millipore, Billerica, MA) and stored at 4° C until further use.

Labeled genomic DNA was hybridized onto cDNA microarrays that were constructed using PCR-amplified gene products of ~95% of *S. cerevisiae* ORFs (M.S. Thesis, Sangurdekar, 2006). Hybridizations were carried out using the standard protocol for cDNA microarrays for wild type and mutant DNA in a dye-swap configuration (Khodursky et al., 2003). The arrays were incubated in a 65°C water bath for 5.5 h and were then washed and scanned on a GenePix scanner. The raw data was extracted using GenePixPro 3.0 software.

Plasmid Construction

Standard molecular biology protocols were followed during the construction of the expression vectors (Sambrook et al., 1989). The centromeric *S. cerevisiae* plasmid pRS169 (Sikorski and Hieter, 1989), which contains the ARS1 origin of replication and the *URA3* gene for selection in yeast auxotrophic for uracil, has *Xho*I and *Eco*RI restriction sites in the multiple cloning site. The gene *LPP1* was cloned from S288c using PCR with primers NNNNNCTCGAGGGAA-ACTCGTCATATTCTA and NNNNNGAATTCCTAAACA-CTAACCGGTGA. The gene was inserted into the aforementioned restriction sites forming the plasmid pRS169-LPP1, which expresses the *LPP1* gene under control of the GAL1 promoter. The GAL1 promoter is inducible by cultivation on galactose as sole carbon source. The plasmid was transformed into *S. cerevisiae* strain D603. A strain transformed with the original plasmid was used as a control. Transformations were performed using standard transformation protocols (Hill et al., 1991). Both plasmids were stored long term in *Escherichia coli* strain DH5-α.

Specific Growth Rate Determination

Single colonies were isolated and cultivated on 5 mL of SD medium in 15 mL tubes overnight with shaking at 30°C, unless otherwise specified. Cultures were transferred to 250 mL Erlenmeyer flasks containing 50 mL of the experimental medium and cultivated to mid-exponential phase with shaking. The experimental medium was either SD or SD supplemented with ethanol or acetate as specified. Cells were then diluted into new flasks containing 50 mL of fresh experimental medium. Growth was monitored for approximately 8 h via optical density, which was measured in acryl cuvettes (1 cm path length) on a spectrophotometer at 600 nm (Hewlett Packard 8452a Diode Array Spectrophotometer, Palo Alto, CA). The specific growth rate was defined as the slope of a line of a semi-log plot of optical density versus time during exponential growth. Specific growth rates were determined from triplicate experiments and error bars reported are the standard deviation of those replicates.

Kinetics of Growth and Ethanol Production in Controlled Bioreactors

Kinetic studies were performed in 10 L Braun bioreactors (Biostat MD, B. Braun Biotech International, Melsungen, Germany), which were maintained at 30°C, operated with a working volume of 6 L, agitated at 300 rpm, and aerated at 0.7 L/min. Bioreactor medium contained 100 g/L glucose, 6.7 g/L yeast nitrogen base without amino acids, and 46.1 g/L sodium acetate trihydrate such that total acetate concentration was 20 g/L total acetate. The pH was controlled at pH 5.6 using 6 M KOH as necessary. Inoculum cultures were cultivated overnight in 250 mL Erlenmeyer flasks with 100 mL of SD medium. All bioreactors were inoculated such that the initial optical density ($OD_{600\ nm}$) was 0.1. The dissolved oxygen (DO) was monitored using a polarographic DO probe (Woburn, MA) and always remained above 40% of saturation. The exhaust gas from the bioreactor was passed through an exhaust gas condenser, then filtered, and finally analyzed by a Prima δ-B mass

spectrometer (ThermoOnix, Houston, TX) to determine the exhaust gas composition. Biomass concentration was determined via optical density and converted to cell dry weight concentrations via gravimetric calibration.

Analytical Techniques

Samples from the batch cultures were taken, placed in 1.5 mL Eppendorf tubes, and centrifuged at 13,000 rcf for 2 min. The supernatants were recovered and the concentrations of glucose, acetate, glycerol, and ethanol were determined using a HPLC system (Shimadz10A, Shimadzu, Columbia, MD) equipped with an autosampler (SIL-20AC), a cation exchange column (HPX-87H, Biorad Labs, Hercules, CA) and two detectors in series including a UV–Vis detector (SPD-20AV) and a refractive index detector (RID-10A). Samples of culture supernatants were first filtered to remove particulates using a 0.22 μm polyethersulfone filter membrane (Fisher Scientific, Hanover Park, IL). Then 10 μl of each sample was loaded into the column, maintained at 65°C. The mobile phase was 5 mM H_2SO_4 and ran isocratically at a flow rate of 0.5 mL/min. The concentration of acetate was quantified from the signal obtained at 210 nm by the UV–Vis detector while the concentrations of glucose, glycerol, and ethanol were quantified from the signal obtained by the refractive index detector.

Results

Effect of Acetate

The effect of acetate on the growth behavior of *S. cerevisiae* was evaluated in the cytostat by applying selected growth conditions. The bioreactor initially contained 0 g/L acetate such that the uninhibited specific growth rate in the cytostat ($\mu = 0.35\ h^{-1}$) could be determined for comparison. The feed medium was changed 5 times, with the culture allowed to reach an apparent steady state before the next feed medium containing higher acetate concentrations was introduced. Figure 1A shows the dilution rate and the mean forward scatter intensities of single cells, which correlates with cell size, as a function of time. By averaging the data acquired during the apparent steady states, we determined the specific growth rate and cell size for each acetate concentration (Fig. 1B). The specific growth rate in the cytostat initially increases with the additional acetate in the feed medium until 5 g/L acetate is supplemented. At concentrations above 5 g/L acetate, the measured specific growth rate in the cytostat decreased linearly with increasing acetate concentrations. The specific growth rate at 14.5 g/L acetate was predicted to equal half the specific growth rate measured at 5 g/L acetate using a linear model of growth inhibition for acetate concentrations above 5 g/L. In addition the mean cell size increases linearly with increasing acetate concentration.

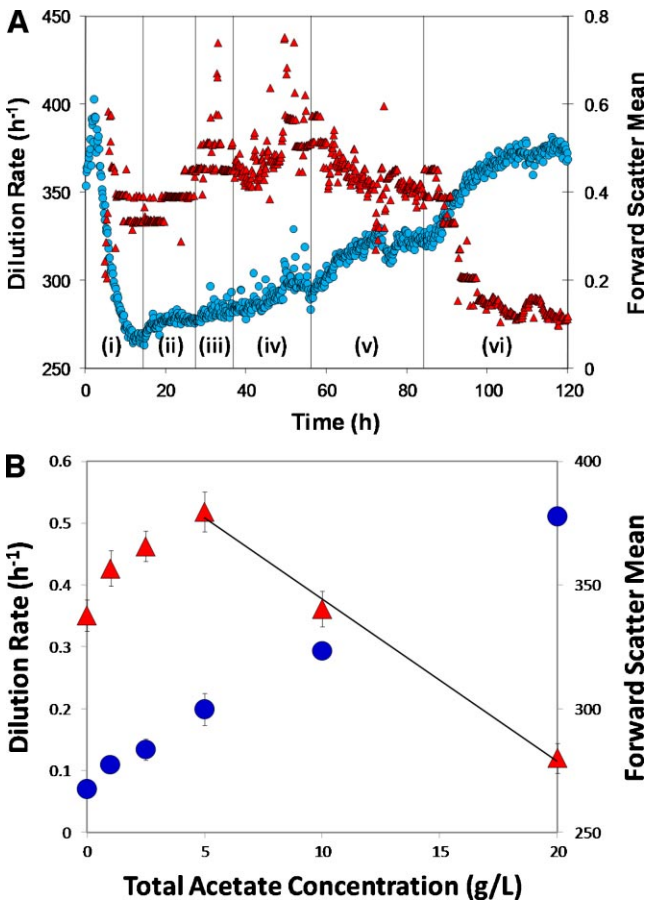

Figure 1. Size and growth rate changes in response to changing acetate concentrations. **A**: The acetate is increased gradually from (i) 0 g/L, (ii) 1 g/L, (iii) 2.5 g/L, (iv) 5 g/L, (v) 10, and (vi) 20 g/L acetate. The vertical lines indicate a transition in acetate. The dilution rate (red triangles) remains high until the 20 g/L acetate feed is introduced. As the acetate concentration increases, the average size as measured by the forward scatter mean (blue circles) increases. **B**: Steady state effects on the specific growth rate and size as measured by forward scatter. The error bars indicate the standard deviation from the apparent steady states immediately prior to the transition in acetate. The solid line models the growth inhibition by acetate, and the equation of the line is $\mu = -0.0263 \times [\text{Acetate}] + 0.640$, which fits the data with a correlation $R^2 = 0.995$. [Color figure can be seen in the online version of this article, available at www.interscience.wiley.com.]

Mutant Enrichment

To rapidly enrich the culture for strains with improved growth phenotypes, culture operation was continued with 20 g/L acetate in the feed medium as the specific growth rate approximates the optimal strategy for isolating mutants, which requires operation of the cytostat to be at 21–34% of the uninhibited specific growth rate (Fig. 2) (Gilbert and Srienc, 2009). The mutant strain displaces the wild type strain within only 3 days of introduction of the 20 g/L acetate feed as indicated by the increase in dilution rate

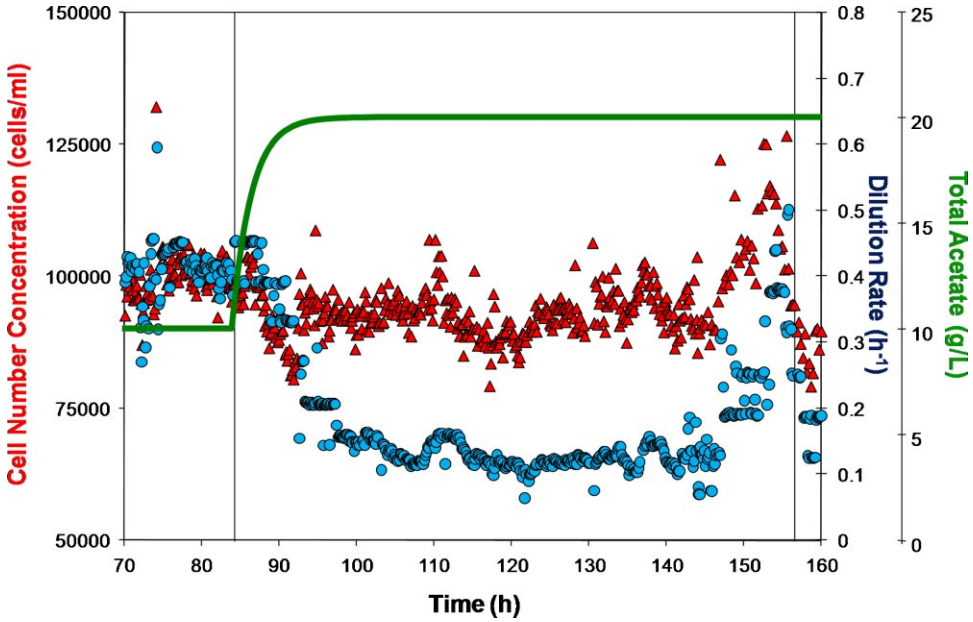

Figure 2. Isolation of strain AG3 in the cytostat under acetate selection. The 20 g/L total acetate (green line) feed is introduced at 84 h and the extracellular environment slowly increases in acetate concentration. The dilution rate (blue circles) and cell concentration (red triangles) decrease as a result of the inhibition of the acetate. The set point is 100,000 cells mL^{-1} and the dilution rate is approximately 0.1 h^{-1}. The mutant AG3 takes over the culture by 155 h at which time the cytostat effluent was plated on agar plates. A single colony then was isolated off the agar plate to yield strain AG3. [Color figure can be seen in the online version of this article, available at www.interscience.wiley.com.]

required to control the culture at the cell concentration set point. The effluent of the cytostat sampled at 155 h was plated and single colonies were isolated. Three colonies were screened for the mutant phenotype of improved specific growth rate in high acetate containing medium. All colonies had a higher specific growth rate than the wild type in the acetate containing medium. The screened colony with the highest specific growth rate was retained (strain AG3) and is isogenic to S288c except for the mutations accumulated during cytostat operation.

Mutant AG4 was enriched in a cytostat from the same parent, S288c, with feed medium always containing the optimal 20 g/L total acetate (Fig. 3). In this enrichment, the initial cell density was above the set point and the feed pump quickly reduced the cell concentration to the applied set point of 450,000 cells mL^{-1}. A distinct shift in the growth is seen after approximately 4 days of cytostat operation when mutant AG4 had become significantly enriched. Another mutant, AG5, was isolated from the parent of opposing mating type, X2180-1A (Mortimer and Johnston, 1986), using the same conditions as with AG4 (data not shown).

The mutant enrichment shown in Figure 2 was performed with tight control of the cell number concentration and little variability in the dilution rate. This control was achieved by changing the feed rates only in discrete steps. As a result, small changes in cell concentration did not result in changes in flow rate. The dilution rate shown in Figure 3 exhibits more variability with respect to that seen in Figure 2 as the medium flow rate was allowed to change continuously in response to changes in cell concentration.

Size Distributions as an Indicator for Population Composition

Because resistant cells are smaller than the acetate sensitive cells in acetate containing medium, the flow cytometry data indicates when resistant cells take over the population. The transients in forward scatter mean and coefficient of

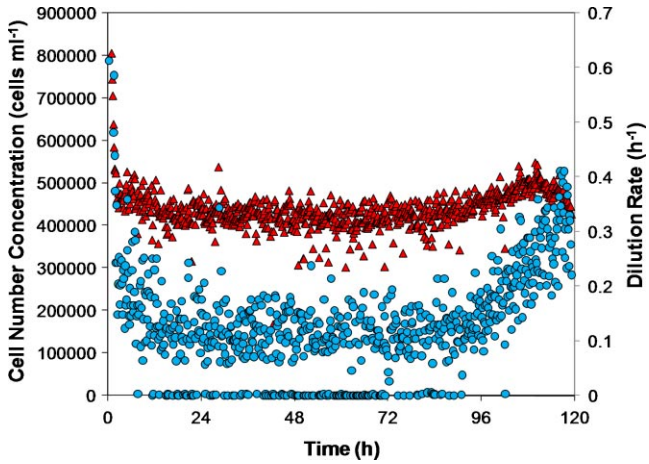

Figure 3. Isolation of strain AG4 in the cytostat under acetate selection. In this case, 20 g/L of acetate is introduced immediately in the feed. The cell concentration (red triangles) is maintained at approximately 450,000 cells mL^{-1}, and the dilution rate (blue circles) is stable at approximately 0.1 h^{-1}. The mutant AG4 has displaced the wild type prior to 120 h. [Color figure can be seen in the online version of this article, available at www.interscience.wiley.com.]

variation (CV) for the cytostat experiment shown in Figure 3 are reported in Figure 4a. The large cell size at steady state in Figure 4a correlates directly to the large cell size observed in Figure 1 in response to the 20 g/L acetate present. At 96 h, the cell concentration and dilution rate are still close to the steady state values (Fig. 3), but the mean forward scatter was already significantly decreased (Fig. 4a), indicating a change in the population composition. Simultaneously, the CV increases which indicates that the population has become more heterogeneous.

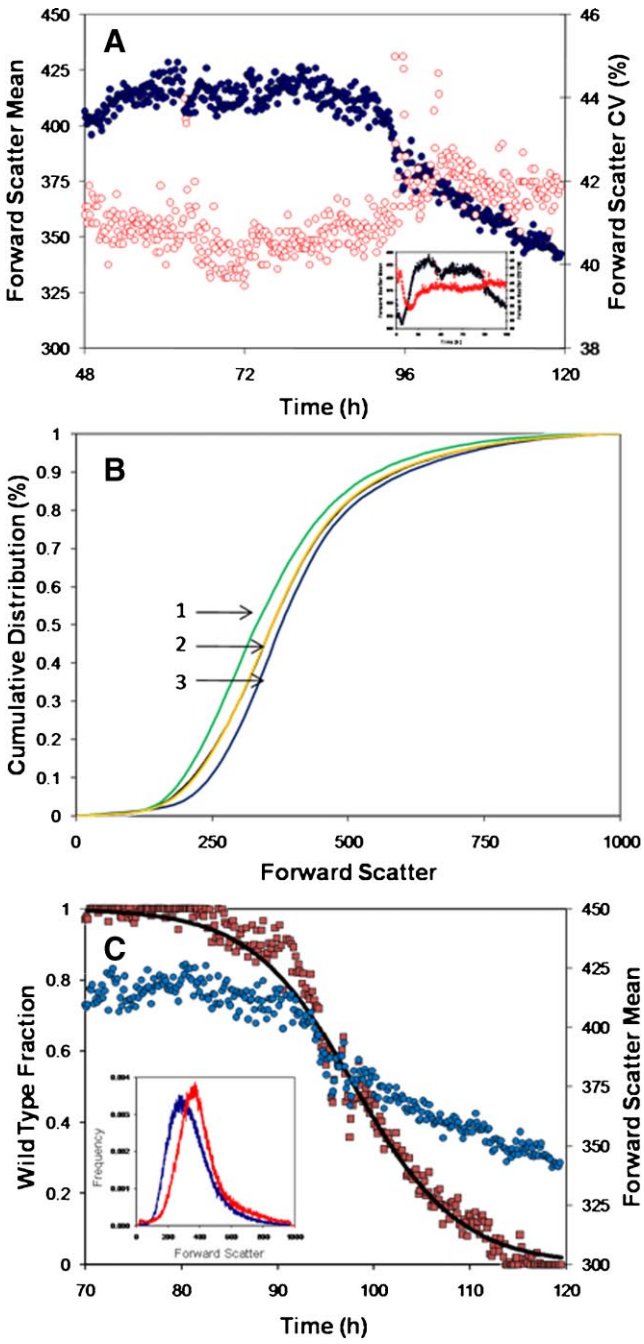

Analysis of the forward scatter cumulative distribution functions (Fig. 4b) over time demonstrate that mutant enrichment results in an accumulation of small cells. We used the transition in size as an indicator of the mutant enrichment. The wild type culture fraction was determined from the measured size distribution using a least squares fit to a weighted sum of the wild type and mutant size distributions. The wild type size distribution was defined as the average of 10 consecutive distribution measurements taken approximately 67 h after inoculation. Similarly, the mutant size distribution was defined as the average of 10 consecutive samples taken at approximately 114 h. By 95 h, already over 40% of the culture is predicted to be mutants even though the deviation in cell concentration from the set point and dilution rate from the steady state at this time is still small. The results of the entire transition from a wild type culture to a mutant culture are shown in Figure 4c. The difference between the wild type and mutant specific growth rates defines the rate of displacement of the wild type cells as described in the theory developed in the Supplemental Material. Using the measured wild type and mutant specific growth rates in the cytostat, the time course of mutant fraction (Fig. 4c) was predicted according to the theory. The agreement between the predicted transient based on first principles and the transient based on light scattering validates this approach for estimation of the population composition. The time course of the transient size distributions is also provided in the Supplementary Material and visualizes the population dynamics.

Mutant Phenotype

The mutants were tested for growth characteristics in stress conditions (Table I). The haploid mutants all grew approximately at a specific growth rate of 0.26 h^{-1} in the presence of 20 g/L acetate, which was a rate over 70% faster

Figure 4. Transients in light scattering properties due to mutant enrichment. **A**: Mutant AG4 takes over the population during cytostat operation. The forward scatter mean (blue circles) and forward scatter coefficient of variation (CV, red open circles) change substantially by 96 h and indicate the mutant takeover. The average mutant cell has a lower average forward scatter than the average wild type cell. The inset depicts the transient behavior for the entire experiment. **B**: Cumulative distribution functions of forward scatter over time. The cells are initially nearly all wild type cells at steady state (labeled 1, green, 70 h). Eventually the mutants start to take over the population (labeled 2, black, 95 h) until the population is almost exclusively mutant cells (labeled 3, blue, 110 h). A least squares fit (yellow), representing a culture 61.3% wild type cells at 95 h, is overlaid and demonstrates excellent agreement between the weighted distribution and the experimental distribution. **C**: Transient in wild type fraction extracted from the forward scatter data. The experimental forward scatter distribution was compared to a weighted sum of the steady state wild type and mutant distributions, and the weight resulting in the minimum error in a least squares fit was selected. The weight indicated the wild type fraction (red squares) of the culture. The forward scatter mean (blue circles) is overlaid such that the changes in culture fraction can be easily compared to the changes observed in cell size. The solid black line indicates the agreement between the extracted fractions and the prediction according to theory and the experimentally measured specific growth rates. The insert depicts the wild type (red) and mutant (blue) distributions used for the least squares fit. [Color figure can be seen in the online version of this article, available at www.interscience.wiley.com.]

Table I. Summary of specific growth rates under various challenges.

	S288C	AG3	AG4	AG5	AG3 × AG5	AG4 × AG5
SD medium	0.40 ± 0.00	0.40 ± 0.01	0.38 ± 0.01	0.36 ± 0.00	0.38 ± 0.01	0.41 ± 0.01
SD medium + 50 g/L ethanol	0.03 ± 0.01	0.08 ± .01	0.08 ± 0.01	0.09 ± 0.00	0.08 ± 0.00	0.10 ± 0.01
SD medium + 20 g/L acetate	0.15 ± 0.00	0.26 ± 0.01	0.26 ± 0.01	0.25 ± 0.02	0.25 ± 0.00	0.33 ± 0.02
SD medium, 37°C	0.29 ± 0.02	0.37 ± 0.02	0.4 ± 0.01	0.35 ± 0.00	0.35 ± 0.01	0.38 ± 0.00

Error bars are reported from triplicate measurements. All growth conditions are at 30°C unless otherwise stated, and all growth rates are measured in h^{-1}.

than the wild type ($\mu = 0.15\ h^{-1}$). The mutants also have faster growth rates as compared to the wild type under the stress conditions of elevated ethanol concentrations and temperature. In fact, the haploid mutants decreased in growth rate at 37°C by less than 7% of the specific growth rate measured at 30°C, while the parental specific growth rate was reduced by 28% under the same conditions.

To test possible additive effects of the mutations, AG5 was crossed with AG3 and AG4 to construct the heterozygous diploid mutants, AG3 × AG5 and AG4 × AG5. The diploid AG3 × AG5 did not have a distinct growth advantage over the individual haploids strains. In contrast the diploid AG4 × AG5 grew 27% faster than AG4 and AG5 and 120% faster than the haploid wild type S288c under acetate stress. Furthermore the diploid AG4 × AG5 appeared to be the most robust strain with a high specific growth rate across all stresses tested (Table I).

A fast growth rate is usually reflected in a larger mean cell size and in a lower fraction of cells in the G1 cell cycle phase. However, the mutant strains had higher specific growth rates and lower average cell sizes than the slower growing wild type under acetate stress. AG3 was chosen for further characterization of the cell cycle distribution under acetate stress. Figure 5 compares the cell cycle distributions of AG3 and S288c, cultivated as described in materials and methods in both minimal medium and minimal medium supplemented with 20 g/L acetate. As can be clearly seen from the DNA distributions (Fig. 5), the slow, inhibited growth of S288c in minimal medium containing acetate was reflected in a larger fraction of the cells in the G1 phase of the cell cycle (48 ± 1% in G1) as compared to growth in minimal medium lacking acetate (29 ± 2% in G1). AG3 essentially has identical cell cycle distributions in the two media (43 ± 1% in G1 in acetate, 39 ± 2% in G1 without acetate). Again, this effect is in contrast to expected size effects in response to growth rates as a slower specific growth rate typically is associated with an accumulation in G1 and smaller cell sizes.

Estimation of the Beneficial Mutation Probability

Assuming that no mutants are present at the time when growth inhibition is imposed on the culture, we can compute the growth dynamics of the wild type and mutant mixed culture using the previously developed model (Gilbert and Srienc, 2009). Since the specific growth rates of mutant and wild type strains and overall cell density are known from experiments, the beneficial mutation probability, or the probability that a given mutation is advantageous to its host, can be varied in silico such that the theoretical enrichment kinetics match the experimental enrichment dynamics. If in reality some mutant cells were initially present, a higher probability than the true beneficial mutation probability would be determined by the model as a higher rate of mutant production would be required to achieve the enrichment in the appropriate total time. Thus the apparent beneficial mutation probability determined here represents the upper limit of the true beneficial mutation probability.

Table II summarizes the cell concentrations and specific growth rates determined in the cytostat experiments as well as the apparent beneficial mutation probabilities extracted based on this approach. The experimental parameters are the average values of the parameter determined from approximately 20 h of steady state growth. From this analysis, we find an apparent beneficial mutation probability of greater than 10^{-8} (beneficial mutations) $cell^{-1}$ (doubling time)$^{-1}$ for the enrichments of AG4 and AG5. This beneficial mutation probability has been determined for *S. cerevisiae* previously (Magni and Von Borstel, 1962; Zeyl and DeVisser, 2001). We also conclude that mutant AG3 likely was present before the 20 g/L acetate feed was introduced to the cytostat as the beneficial mutation probability determined for isolation of AG3 was substantially higher than in the other two isolations. According to the theoretical calculations, it is likely that AG3 had accumulated to approximately 15,000 total cells, or 0.046% of population, by the time the 20 g/L feed medium was introduced. Continuous cultivation for 84 h prior to the introduction of the 20 g/L feed medium likely only changed the total number of cultivation hours required for mutant isolation.

Kinetics of Growth and Product Formation

The practical result of this work was the construction of robust strains capable of producing ethanol at high rates and titers in the presence of severe inhibition by acetate. We compared the strains produced in this study to their parental strain and to a commercial ethanol producing strain, Ethanol Red (Fermentis, Marcq-en-Barœul, France), under identical conditions. The results from the ethanol

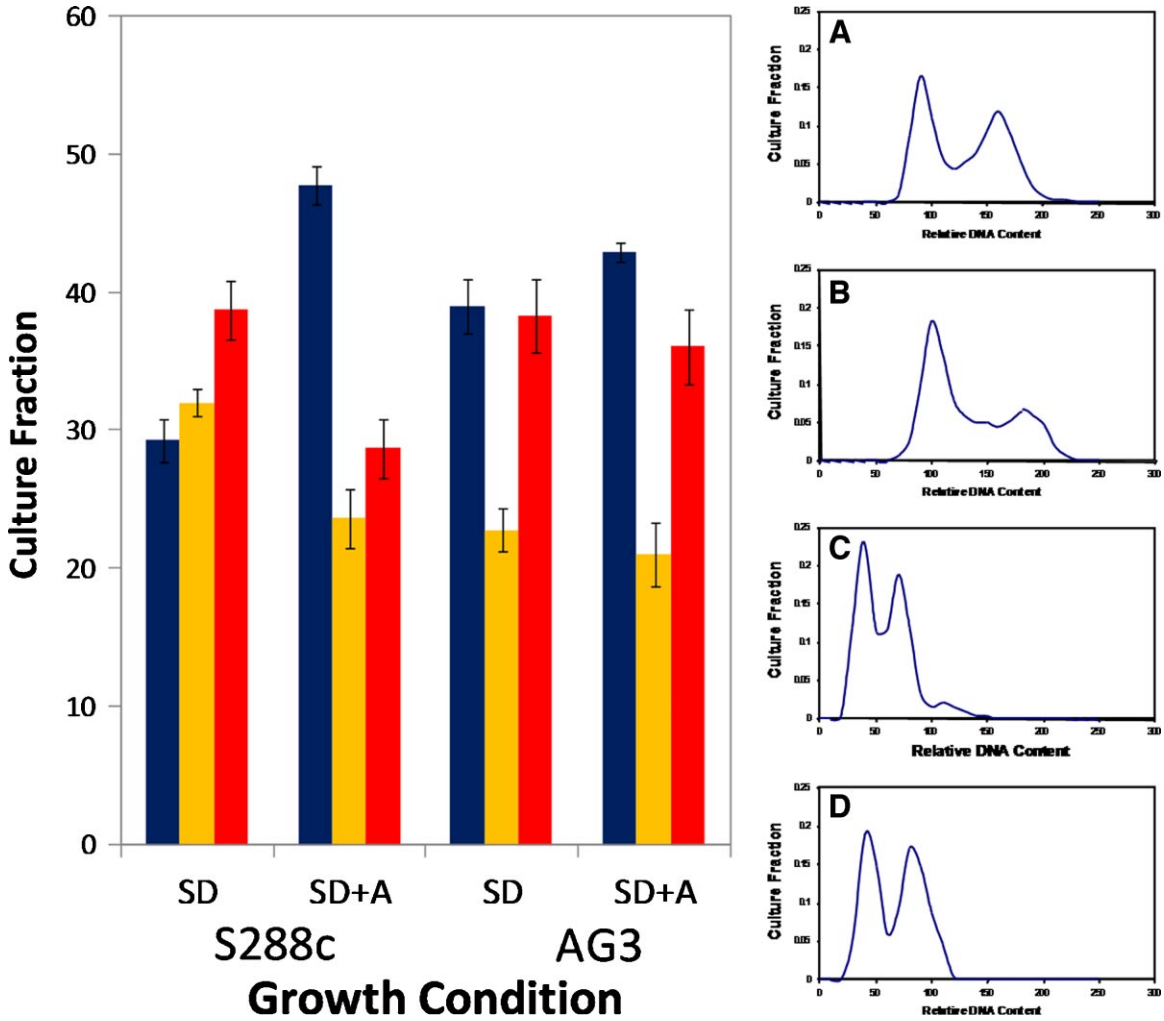

Figure 5. Cell cycle distributions for strains S288c and AG3 in SD minimal medium and SD minimal medium containing 20 g/L acetate (SD + A). From left to right, the cell cycle phases are G1 (blue), S (orange), and G2 + M (red). The cell cycle distributions were measured after 4 h of incubation in fresh medium as described in Materials and Methods Section, and error bars are the standard deviation of triplicate experiments. The side panel **A** represents the DNA distribution measured for S288c in medium without acetate, **B** represents the data for S288c in medium with acetate, **C** represents AG3 in medium without acetate, and **D** represents AG3 in medium with acetate. [Color figure can be seen in the online version of this article, available at www.interscience.wiley.com.]

production studies, performed in identical conditions in controlled aerobic bioreactors, are summarized in Table III. Aerobic conditions results in high ethanol productivity (Alfenore et al., 2004) and a substantial amount of data under such conditions can be found in the literature for comparison (Locher et al., 1993; Nissen et al., 2000; Ostergaard et al., 2000; Hantelmann et al., 2006; Rudolf et al., 2007; Van Vleet et al., 2008).

The mutant strains collectively exhibited higher ethanol yields and titers than either the wild type or the industrial organism. In fact, the mutant strains achieve ethanol yields in the presence of 20 g/L acetate similar to the ethanol yields

Table II. Summary of mutant strain isolations using the cytostat.

Wild type strain	Mutated strain	Mating type	Cell density (cells/mL)	Wild type specific growth rate (h^{-1})	Mutant specific growth rate (h^{-1})	Cytostat volume (mL)	Isolation time (h)	Beneficial mutation probability
S288c	AG3	α	95,100	0.12	0.26	345	71	$>10^{-6}$
S288c	AG4	α	420,000	0.075	0.26	310	110	5×10^{-8}
X2180-1A	AG5	a	443,000	0.098	0.26	390	110	8×10^{-8}

Beneficial mutation probabilities are the best fit based on model simulations of mutant isolation (Gilbert and Srienc, 2009). The isolation time is defined as the elapsed time from introduction of the selection pressure. The cell densities, specific growth rates, volumes, and isolation times listed are those values used in the model simulations.

Table III. Summary of controlled bioreactor experiments.

	S288C	AG3	AG4	AG5	AG3 × AG5	AG4 × AG5
Ethanol yield	0.32	0.37	0.41	0.39	0.39	0.40
Acetate yield	0.014	0.009	0.008	0.009	0.007	0.008
Glycerol yield	0.061	0.051	0.041	0.038	0.034	0.038
Time required	120.92	70.75	61.50	63.75	63.83	54.33
Biomass titer	1.33	1.95	2.33	2.15	2.48	2.83

All bioreactors were performed in identical conditions with minimal medium containing 100 g/L glucose, 6.7 g/L yeast nitrogen base without amino acids, and 20 g/L total acetate at pH 5.6. All yields are reported as the total product divided by the total glucose consumed. The time required reported is the elapsed time for ethanol production. AG4 × AG5 has the shortest time required due to its enhanced growth properties. The biomass titer is reported in g cell dry weight/L as determined by gravimetric calibration with optical density. As the HPLC is accurate down to the mg/L range and g/L quantities are produced or supplied for ethanol, acetate, glycerol, and glucose, the error in determining the yields is not significant.

obtained in the literature under uninhibited conditions (Locher et al., 1993; Nissen et al., 2000; Ostergaard et al., 2000; Hantelmann et al., 2006; Rudolf et al., 2007; Van Vleet et al., 2008). Of all the mutants, strain AG4 × AG5 has the highest ethanol volumetric productivity. This is due to the growth advantage available to the strain, and its ability to reach the highest biomass concentration. The kinetics of growth, glucose consumption, and ethanol production for strains AG4 × AG5, Ethanol Red, and S288c are shown in Figure 6A and B and clearly demonstrate the higher ethanol production rate of AG4 × AG5. Local specific rates also were determined and are defined as the local rate of change divided by the biomass concentration. AG4 × AG5 reached higher local specific rates of glucose consumption, ethanol production, and growth than either Ethanol Red or S288c (Fig. 6C–E). Analysis of the local specific rates indicated that specific ethanol production and specific glucose consumption were relatively independent of growth rate. Therefore the ethanol produced and glucose consumed were largely non-growth associated. While the industrial strain (Ethanol Red) produced ethanol substantially faster than S288c, Ethanol Red only produced 88% of the ethanol made by AG4 × AG5 and required 27% more time. The mutants' high ethanol yield is partially due to the decrease in secretion of other undesirable side products as compared to the wild type strain (Table III). The mutant strains produced less glycerol than both the industrial and the wild type strain. In all strains tested, glycerol is the dominant undesired byproduct. Although the mutants do produce more acetate than the industrial strain, the increase in acetate production is marginal. While the mutant strains produce ethanol at similar rates to the parental strains and at lower rates than Ethanol Red in medium lacking acetate (data not shown), the mutant strains have superior ethanol production rates in medium containing acetate.

Identification of Mutations at the Genome Level

To identify mutations which confer tolerance, we performed comparative genome hybridization (CGH) studies on DNA microarrays to interrogate the differences between AG3, AG4, AG5, and S288c. CGH is a standard technique, frequently used in the literature to identify changes in gene copy number (Dunham et al., 2002; Dunn et al., 2005; Gerstein et al., 2006; Pollack et al., 1999). Unfortunately, these CGH studies only detect large scale changes at single-gene resolution and cannot detect point mutations. Using the standard technique of significance analysis of microarrays (SAM) (Tusher et al., 2001), only one ORF (YDR503C/LPP1) was found to be significantly different in AG3 out of all ORFs on the array. This gene was found to be over-represented in AG3 at an average of 2.5-fold over the different replicates, with a false discovery rate of 0%, as reported by SAM. No other gene was reported to be significantly different on this platform. AG4 and AG5 were both found to have more than twofold amplifications in three ORFs (YDR038C/ENA5, YDR039C/ENA2, YDR040C/ENA1), each with a false discovery rate of 0% (Fig. 7). Example intensity plots are presented in Figure 7.

Overexpression of *LPP1*

To test whether the amplification of *LPP1* leads to acetate tolerance, a multicopy plasmid, with expression of *LPP1* under control of a galactose inducible promoter, was transformed into strain D603. The strain overexpressing *LPP1* on the plasmid grows indeed faster on galactose in the presence of acetate than D603 harboring the backbone plasmid as a control (Fig. 8). Therefore the data suggest that *LPP1* is likely involved in the phenotype of acetate tolerance. Because of the involvement of three genes, a similar experiment with the set of *ENA* genes has not been carried out yet.

Discussion

Through the use of the cytostat, mutant strains were isolated within only a few days. Standard mutant isolation techniques, including chemostats and serial dilution, require upwards of 40–100 generations (Adams et al., 1985; Hegreness et al., 2006; Joachimsthal et al., 1998; Kuyper et al., 2005), while the cytostats shown here required fewer than 20. More generations are required in standard techniques as typically high cell densities are used, resulting in poor nutritional environments, lower specific growth rates, and small growth advantages for the mutants over the parental strains. The cytostat cultures grow at low cell densities and the maximum specific growth rate supported by the feed medium, leading to larger absolute growth advantages for the mutants over the parental strains. The result is fewer generations are required, and the generations occur on a shorter time scale. Even in cases where the genetic modifications for tolerance are known, cytostat technology, resulting in mutant isolation in only a few days, is extremely competitive with the time requirements of standard

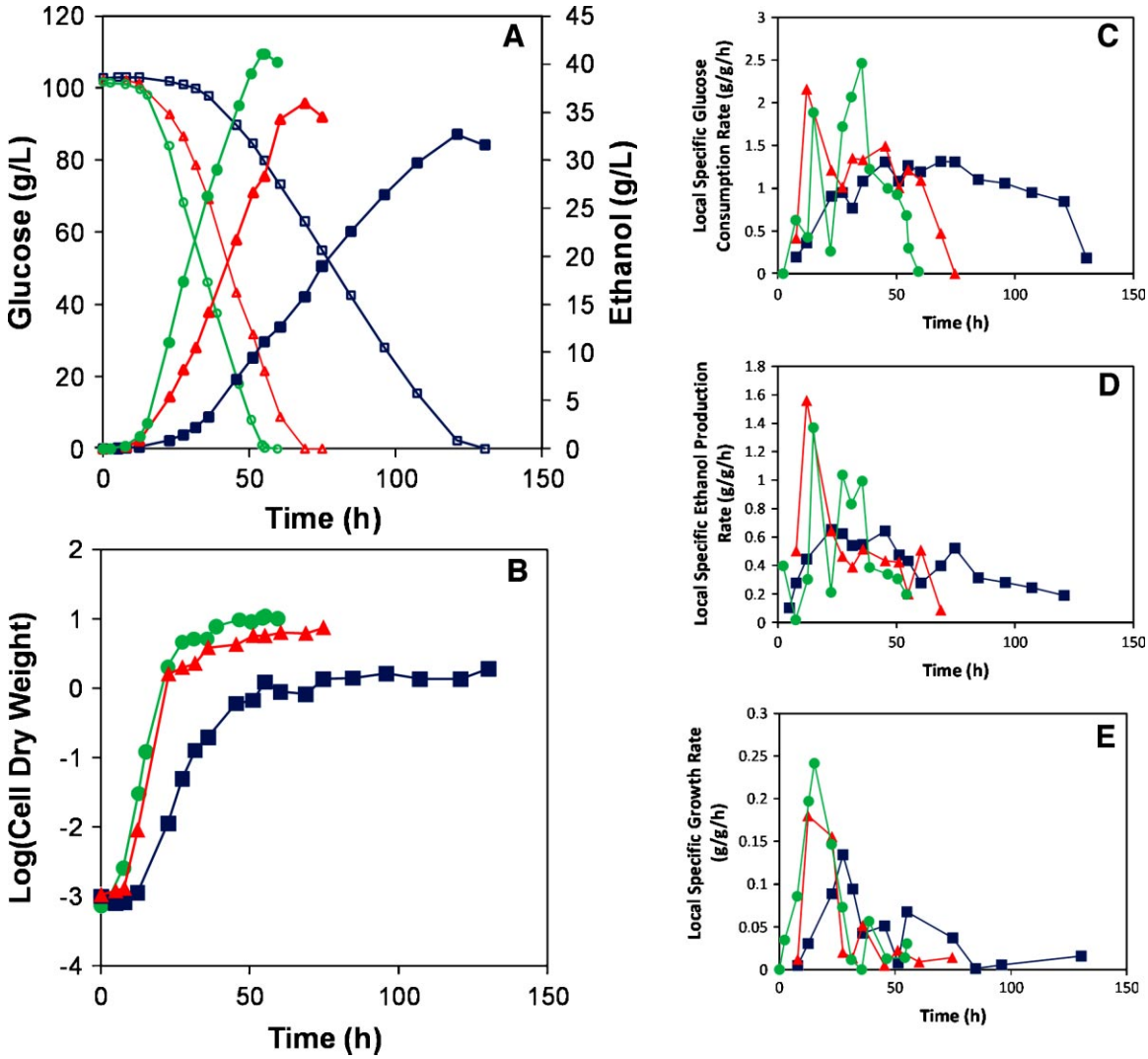

Figure 6. Growth and product formation kinetics in acetate containing medium. These experiments were carried out in controlled bioreactors with a 6 L working volume at 30°C, pH 5.6, agitation rate of 300 rpm, and aeration rate of 0.7 vvm. In all panels, green circles refer to the diploid mutant AG4 × AG5, red triangles refer to the industrial ethanol producer Fermentis Ethanol Red, and blue squares refer to the wild type S288c. **A**: AG4 × AG5 produces ethanol more quickly than both Ethanol Red and the wild type S288c. AG4 × AG5 consumes glucose (open symbols) at the fastest rate and produces the highest ethanol titer (closed symbols) in minimal medium supplemented with 20 g/L acetate. **B**: Strain AG4 × AG5 grows faster and reaches a higher biomass titer than Ethanol Red and the wild type S288c. Cell dry weights were determined by gravimetric correlation with optical density. **C**: The local specific glucose consumption rate, defined as the local rate of change of biomass, reached a higher rate for AG4 × AG5 than for Ethanol Red and S288c. **D**: The local specific ethanol production rate, defined as the local rate of change of ethanol concentration divided by the biomass concentration, was at a higher rate for approximately 20 h for AG4 × AG5 than for Ethanol Red and the wild type S288c. **E**: The local specific growth rate, defined as the local rate of change of biomass, reached a higher rate for AG4 × AG5 than for Ethanol Red and the wild type S288c. [Color figure can be seen in the online version of this article, available at www.interscience.wiley.com.]

molecular biology techniques. Cytostat technology also has the advantage of utilizing the native genome of the organism, such that phenotypic improvements are likely to be stable with comparison to improvements conferred by recombinant nonnative genes.

ENA1, *ENA2*, and ENA5 are three sequential genes, which are present on chromosome IV and encode for P-type ATPase sodium pumps (Hirayama et al., 1995). *ENA1*, *ENA2*, and *ENA5* have previously been shown to confer salt, pH, and osmolarity tolerance to *S. cerevisiae* (Hirayama et al., 1995; Ruiz and Arino, 2007). Deletions of these genes also lead to sensitivity to salt tolerance (Mendizabal et al., 1998). Due to the variety of tolerances associated with expression of these genes and the fact that two strains were isolated with the same gene amplifications, we conclude that overexpression of these genes leads to increased tolerance to acetate, temperature, and ethanol in strains AG4 and AG5.

LPP1 amplification in strain AG3 also appears to confer acetate, ethanol, and temperature tolerance. *LPP1*, a lipid phosphate phosphatase also present on chromosome IV, accepts a variety of substrates including phosphatidic and

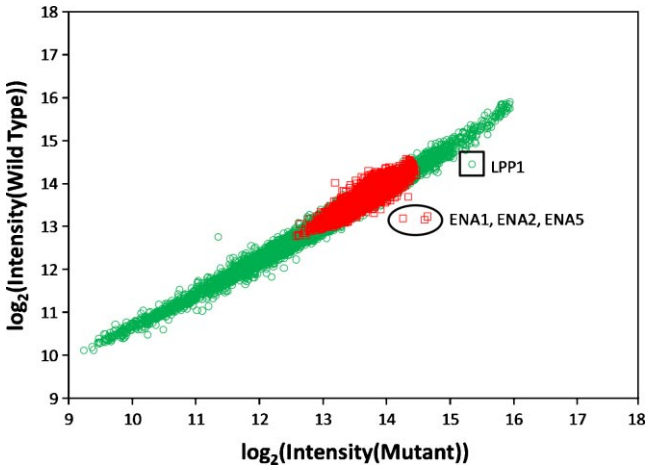

Figure 7. A typical intensity scatter plot comparing wild type and mutant genomic DNA intensities. All of the intensities fall along the expected diagonal line, indicating no change in genomic copy number. In the comparison of strain AG3 (green circles) with S288c, only *LPP1* is significantly different. This spot is highlighted with a box, and the data point falls below the diagonal indicating an amplification in the mutant strain of this gene. In the comparison of strain AG4 (red squares) with S288c, *ENA1*, *ENA2*, and *ENA5* are significantly different. This spot is highlighted with an oval. [Color figure can be seen in the online version of this article, available at www.interscience.wiley.com.]

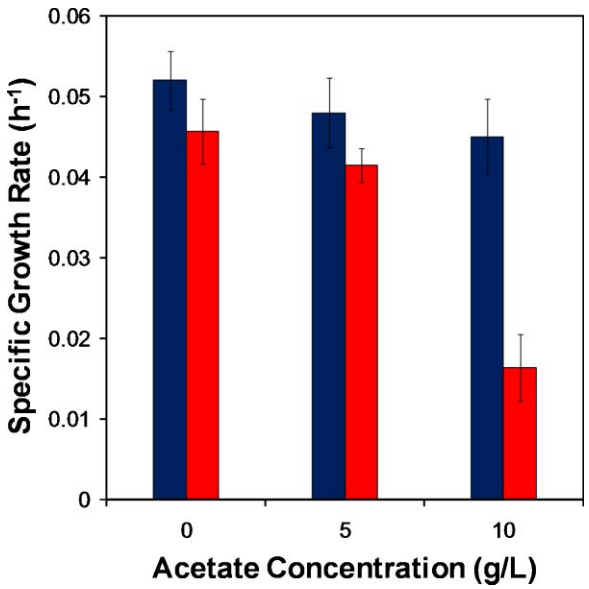

Figure 8. Overexpression of *LPP1* results in increased acetate tolerance. Yeast strain D603 harboring the backbone vector (red) does not grow as quickly in the presence of acetate as D603 harboring the plasmid expressing *LPP1* (blue). The strain expressing the gene shows essentially no change in specific growth rate while the strain only expressing the backbone vector has a substantial decrease in growth rate. The specific growth rates are all low due to necessary growth on galactose for induction purposes. [Color figure can be seen in the online version of this article, available at www.interscience.wiley.com.]

lysophosphatidic acids (Faulkner et al., 1999; Furneisen and Carman, 2000; Toke et al., 1998). Modification of the relative levels of these substrates, which are major intermediates in lipid metabolism, affects the membrane composition. Ghosh et al. (2008) recently demonstrated that the concentrations of these compounds are increased under organic solvent stress in *S. cerevisiae*. While additional mutations such as point mutations cannot be ruled out, amplification of *LPP1* is the likely cause of the enhanced tolerance to ethanol, acetate, and temperature shown here.

The resulting mutant strains with these amplifications have faster ethanol production kinetics and reach higher ethanol titers than the parental strain. The diploid mutant strain AG4 × AG5 is even more robust than the other mutant strains in terms of acetate tolerance, suggesting that additional amplification of the *ENA* genes is helpful. AG3 × AG5, a combination of the *LPP1* and *ENA* amplifications, is not as tolerant as AG4 × AG5 as the individual mutations present in AG3 and AG5 did not result in another enhancement when combined. This suggests that there may be gene dosage effects and construction of a homozygous diploid from the haploid AG3 may result in a faster specific growth rate in acetate containing medium.

We compared the strains isolated here directly to a robust industrial strain. While the industrial strain is a vigorous ethanologenic strain, the mutant strains produce ethanol at higher titer and productivity in the presence of high acetate concentrations. The mutant strains produce less waste products than the wild type and industrial strains, which is desirable as downstream processing is simpler. Thus the cytostat mutant isolates are very attractive strains as a starting point for cellulosic ethanol production. Further improvements are likely necessary in these strains, including furan and phenolic tolerance and introducing pentose fermentation capabilities, prior to industrial use. As many additional mutations will likely be required in order to produce a desired production strain, the cytostat methodology clearly provides a significant advantage as the length of time required for phenotypic improvements is so short.

As the cytostat is generally applicable to all microorganisms growing in suspension culture, this technique can be applied to a multitude of systems. The evolutionary possibilities available through the cytostat should be used to rapidly improve industrial strains for production of biochemicals, including biofuels. The example of improved acetate tolerance in *S. cerevisiae* demonstrates that this is a feasible method, representing a significant advancement of current technology. In addition, the necessary mutations occur on the basis of the natural mutation rate without the aid of external mutagens. As a result, there is a very clear relationship between the mutations identified and the phenotype. Therefore the knowledge gained from identifying the nature of the mutations can be directly applied to improve other strains through standard molecular biology practices.

We thank Mascoma Corp. for partially supporting this work.

References

Adams J, Paquin C, Oeller PW, Lee LW. 1985. Physiological characterization of adaptive clones in evolving populations of the yeast, *Saccharomyces cerevisiae*. Genetics 110:173–185.

Aden A, Ruth M, Ibsen K, Jechura J, Neeves K, Sheehan J, Wallace B, Montague L, Slayton A, Lukas J. 2002. Lignocellulosic biomass to ethanol process design and economics utilizing co-current dilute acid prehydrolysis and enzymatic hydrolysis for corn stover. NREL/TP-510-32438. Golden, CO: National Renewable Energy Laboratory. http://www.nrel.gov/docs/fy02osti/32438.pdf

Alfenore S, Cameleyre X, Benbadis L, Bideaux C, Uribelarrea JL, Goma G, Molina-Jouve C, Guillouet SE. 2004. Aeration strategy: A need for very high ethanol performance in Saccharomyces cerevisiae fed-batch process. Appl Microbiol Biotechnol 63:537–542.

Berson R, Young J, Kamer S, Hanley T. 2005. Detoxification of actual pretreated corn stover hydrolysate using activated carbon powder. Appl Biochem Biotechnol 124:923–934.

Buhner J, Agblevor F. 2004. Effect of detoxification of dilute-acid corn fiber hydrolysate on xylitol production. Appl Biochem Biotechnol 119:13–30.

Burke D, Stearns T. 2000. Methods in yeast Genetics (A Cold Spring Harbor Laboratory Course Manual). Cold Spring Harbor, NY: Cold Spring Harbor Press.

Dunham MJ, Badrane H, Ferea T, Adams J, Brown PO, Rosenzweig F, Botstein D. 2002. Characteristic genome rearrangements in experimental evolution of *Saccharomyces cerevisiae*. Proc Natl Acad Sci USA 99:16144–16149.

Dunn B, Levine RP, Sherlock G. 2005. Microarray karyotyping of commercial wine yeast strains reveals shared, as well as unique, genomic signatures. BMC Genomics 6:53.

Faulkner A, Chen X, Rush J, Horazdovsky B, Waechter CJ, Carman GM, Sternweis PC. 1999. The LPP1 and DPP1 gene products account for most of the isoprenoid phosphate phosphatase activities in Saccharomyces cerevisiae. J Biol Chem 274:14831–14837.

Furneisen JM, Carman GM. 2000. Enzymological properties of the LPP1-encoded lipid phosphatase from Saccharomyces cerevisiae. Biochim Biophys Acta 1484:71–82.

Gerstein AC, Chun HE, Grant A, Otto SP. 2006. Genomic convergence toward diploidy in *Saccharomyces cerevisiae*. PLos Genet 2(9):e145.

Ghosh AK, Ramakrishnan G, Rajasekharan R. 2008. YLR099C (ICT1) encodes a soluble Acyl-CoA-dependent lysophosphatidic acid acyltransferase responsible for enhanced phospholipid synthesis on organic solvent stress in Saccharomyces cerevisiae. J Biol Chem 283:9768–9775.

Gilbert A, Srienc F. 2009. Optimized evolution in the cytostat: A Monte Carlo simulation. Biotech Bioeng 102:221–231.

Hahn-Hägerdal B, Lindén T, Senac T, Skoog K. 1991. Ethanolic fermentation of pentoses in lignocellulose hydrolysates. Appl Biochem Biotechnol 28–29:131–144.

Hahn-Hägerdal B, Karhumaa K, Fonseca C, Spencer-Martins I, Gorwa-Grauslund M. 2007. Towards industrial pentose-fermenting yeast strains. Appl Microbiol Biotechnol 74:937–953.

Hantelmann K, Kollecker M, Hüll D, Hitzmann B, Scheper T. 2006. Two-dimensional fluorescence spectroscopy: A novel approach for controlling fed-batch cultivations. J Biotechnol 121:410–417.

Hegreness M, Shoresh N, Hartl D, Kishony R. 2006. An equivalence principle for the incorporation of favorable mutations in asexual populations. Science 311:1615–1617.

Hill J, Donald KAIG, Griffiths DE. 1991. DMSO-enhanced whole cell yeast transformation. Nucl Acids Res 19:5791.

Hirayama T, Maeda T, Saito H, Shinozaki K. 1995. Cloning and characterization of seven DNAs for hyperosmolarity-responsive genes of Saccharomyces cerevisiae. Mol Gen Genet 249:127–1138.

Joachimsthal E, Haggett KD, Jang J, Rogers PL. 1998. A mutant of *Zymomonas mobilis* ZM4 capable of ethanol production from glucose in the presence of high acetate concentrations. Biotechnol Lett 20:137–142.

Kacmar J, Srienc F. 2005. Dynamics of single cell property distributions in Chinese hamster ovary cell cultures monitored and controlled with automated flow cytometry. J Biotechnol 120:410–420.

Kacmar J, Gilbert A, Cockrell J, Srienc F. 2006. The cytostat: A new way to study cell physiology in a precisely defined environment. J Biotechnol 126:163–172.

Khodursky AB, Bernstein JA, Peter BJ, Rhodius V, Wendisch VF, Zimmer DP. 2003. Escherichia coli spotted double-strand DNA microarrays: RNA extraction, labeling, hybridization, quality control, and data management. Methods Mol Biol 224:61–78.

Klinke HB, Olsson L, Thomsen AB, Ahring BK. 2003. Potential inhibitors from wet oxidation of wheat straw and their effect on ethanol production of *Saccharomyces cerevisiae:* Wet oxidation and fermentation by yeast. Biotechnol Bioeng 81:738–747.

Kuyper M, Toirkens MJ, Diderich JA, Winkler AA, van Dijken JP, Pronk JT. 2005. Evolutionary engineering of mixed-sugar utilization by a xylose-fermenting *Saccharomyces cerevisiae* strain. FEMS Yeast Res 5:925–934.

Locher G, Hahnemann U, Sonnleitner B, Fiechter A. 1993. Automatic bioprocess control. 4. A prototype batch of *Saccharomyces cerevisiae*. J Biotechnol 29:57–74.

Magni GE, Von Borstel RC. 1962. Different rates of spontaneous mutation during mitosis and meiosis in yeast. Genetics 47:1098–1108.

Mendizabal I, Rios G, Mulet JM, Serrano R, de Larrinoa IF. 1998. Yeast putative transcription factors involved in salt tolerance. FEBS Lett 425:323–328.

Mohagheghi A, Ruth M, Schell DJ. 2006. Conditioning hemicellulose hydrolysates for fermentation: Effects of overliming pH on sugar and ethanol yields. Process Biochem 41:1806–1811.

Mortimer RK, Johnston JR. 1986. Geneaology of principal strains of the yeast genetic stock center. Genetics 113:35–43.

Nissen TL, Hamann CW, Kielland-Brandt MC, Nielsen J, Villadsen J. 2000. Anaerobic and aerobic batch cultivations of *Saccharomyces cerevisiae* mutants impaired in glycerol synthesis. Yeast 16:463–474.

Ostergaard S, Roca C, Rønnow B, Nielsen J, Olsson L. 2000. Physiological studies in aerobic batch cultivations of *Saccharomyces cerevisiae* strains harboring the *MEL1* gene. Biotechnol Bioeng 68:252–259.

Palmqvist E, Grage H, Meinander NQ, Hahn-Hägerdal B. 1999. Main and interaction effects of acetic acid, furfural, and *p*-hydroxybenzoic acid on growth and ethanol productivity of yeasts. Biotechnol Bioeng 63:46–55.

Pampulha ME, Loureiro-Davis MC. 1989. Combined effect of acetic acid, pH and ethanol on intracellular pH of fermenting yeast. Appl Microbiol Biotechnol 31:547–550.

Pollack JR, Perou CM, Alizadeh AA, Eisen MB, Pergamenschikov A, Williams CF, Jeffrey SS, Botstein D, Brown PO. 1999. Genome-wide analysis of DNA copy-number changes using cDNA microarrays. Nat Genet 23:41–46.

Porro D, Brambilla L, Alberghina L. 2003. Glucose metabolism and cell size in continuous cultures of Saccharomyces cerevisiae. FEMS Microbiol Lett 229:165–171.

Rudolf A, Lequeux G, Liden G. 2007. Controlled pilot development unit-scale fed-batch cultivation of yeast on spruce hydrolysates. Biotechnol Prog 23:351–358.

Ruiz A, Arino J. 2007. Function and regulation of the Saccharomyces cerevisiae ENA sodium ATPase system. Eukaryotic Cell 6:2175–2183.

Sambrook J, Fritsch EF, Maniatis T. 1989. Molecular cloning: A laboratory manual. 2nd edn. Cold Spring Harbor, NY: Cold Spring Harbor Laboratory Press.

Sangurdekar D. 2006. Stability and application of principal components analysis in the analysis of multidimensional transcriptional data. M.S. Thesis, University of Minnesota.

Sikorski R, Hieter P. 1989. A system of shuttle vectors and yeast host strains designed for efficient manipulation of DNA in *Saccharomyces cerevisiae*. Genetics 122:19–27.

Srienc F, Campbell JL, Bailey JE. 1986. Flow cytometry analysis of recombinant *Saccharomyces cerevisiae* populations. Cytometry 7:132–141.

Stephanopoulos G. 2007. Challenges in engineering microbes for biofuels production. Science 315:801–804.

Taherzadeh MJ, Eklund R, Gustafsson L, Niklasson C, Liden G. 1997. Characterization and fermentation of dilute-acid hydrolyzates from wood. Ind Eng Chem Res 36:4659–4665.

Toke DA, Bennett WL, Oshiro J, Wu W, Voelker DR, Carman GM. 1998. Isolation and characterization of the Saccharomyces cerevisiae LPP1 gene encoding a Mg2+-independent phosphatidate phosphatase. J Biol Chem 273:14331–14338.

Tusher VG, Tibshirani R, Chu G. 2001. Significance analysis of microarrays applied to the ionizing radiation response. Proc Natl Acad Sci USA 98:5116–5121.

Van Vleet JH, Jeffries TW, Olsson L. 2008. Deleting the para-nitrophenyl phosphatase F (pNPPase), PHO13, S in recombinant Saccharomyces cerevisiae improves growth, ethanol production on d-xylose. Metabolic Eng 10:360–369.

Zeyl C, DeVisser JAGM. 2001. Estimates of the rate and distribution of fitness effects of spontaneous mutation in *Saccharomyces cerevisiae*. Genetics 157:53–61.